The Astronomical Journal, 160:75 (7pp), 2020 August https://doi.org/10.3847/1538-3881/ab9ca2

WIYN Open Cluster Study. LXXXI. Caught in the Act? The Peculiar Red Giant NGC 2243-W2135

Barbara J. Anthony-Twarog[1], Constantine P. Deliyannis[2], and Bruce A. Twarog[1]
[1] Department of Physics and Astronomy, University of Kansas, Lawrence, KS 66045-7582, USA; bjat@ku.edu, btwarog@ku.edu
[2] Department of Astronomy, Indiana University, Bloomington, IN 47405-7105, USA; cdeliyan@indiana.edu
Received 2020 March 19; revised 2020 June 4; accepted 2020 June 13; published 2020 July 23

Abstract

High-dispersion spectra for giants through turnoff stars in the Li 6708 Å region have been obtained and analyzed in the old, metal-deficient open cluster, NGC 2243. When combined with high-dispersion data from other surveys, the cluster is found to contain a uniquely peculiar star at the luminosity level of the red clump. The giant is the reddest star at its luminosity, exhibits variability at a minimum 0.1 mag level on a timescale of days, is a single-lined, radial-velocity variable, and has $v \sin i$ between 35 and 40 km s^{-1}. In sharp contrast with the majority of the red giant cluster members, the star has a detectable Li abundance, potentially as high or higher than other giants observed to date while at or just below the boundary normally adopted for Li-rich giants. The observed anomalies may be indicators of the underlying process by which the giant has achieved its unusual Li abundance, with a recent mass transfer episode being the most probable within the currently limited constraints.

Unified Astronomy Thesaurus concepts: Open star clusters (1160)

1. Introduction

The atmospheric Li abundance (A(Li)[3]) of main-sequence stars between $T_{\rm eff} = 5800$ and 7500 K supplies insight into the internal structure of the majority of stars populating the red giant region of the color–magnitude diagram (CMD) observable today. In broad strokes, the basic outline of the atmospheric evolution is reasonably well understood. At minimum, convection, to varying degrees, depletes the surface Li abundance during the pre-main-sequence phase. Stars observed today as A dwarfs would have depleted almost no Li, while depletion would have been increasingly severe for increasingly lower-mass dwarfs (Pinsonneault 1997). In addition, a large body of evidence suggests that angular momentum loss during the main sequence drives mixing and Li depletion for G dwarfs (e.g., Ryan & Deliyannis 1995), F dwarfs (e.g., Boesgaard et al. 2020), including the striking Li Dip, (Boesgaard & Tripicco 1986), and late A dwarfs alike (Deliyannis et al. 2019, hereafter D19). Thus, nearly all Population I stars enter the subgiant phase with their surface Li depleted by 0.2 to 2 dex or more, depending on mass and other factors.

Subsequent evolution complicates matters further. There is subgiant dilution due to the severe deepening of the surface convection zone, additional nonconvective mixing for low-mass giants past the luminosity bump on the RGB, and possible mixing due to He-ignition at the tip of the red giant branch (RGB). (For an extensive discussion of this complex topic, see D19 and references therein.)

For decades, Li-rich giants (A(Li) > 1.5; see, e.g., Gao et al. 2019 and references therein) have been the exceptions that prove the rule, though the specific mechanism that triggers the Li enhancement has remained elusive. Primary candidates include the Cameron–Fowler (Cameron & Fowler 1971) mechanism operating within asymptotic giant branch stars, enhanced deep mixing operating in first-ascent red giants at the giant branch bump or at He-ignition, and planetary engulfment (see, e.g., Carlberg et al. 2015; Smiljanic et al. 2018; Soares-Furtado et al. 2020, and references therein).

To understand atmospheric Li evolution among low-mass stars, an extensive spectroscopic program has been underway to survey members of a key set of open clusters from the tip of the giant branch to as far down the main sequence as the technology allows. New spectroscopy and/or reanalyses of published data have been discussed for NGC 752, NGC 3680, and IC 4651 (Anthony-Twarog et al. 2009), NGC 6253 (Anthony-Twarog et al. 2010; Cummings et al. 2012), NGC 2506 (Anthony-Twarog et al. 2016b, 2018), Hyades and Praesepe (Cummings et al. 2017), and NGC 6819 (Lee-Brown et al. 2015; Anthony-Twarog et al. 2016a; Deliyannis et al. 2019). Thanks to a sample size of over 300 stars, the analysis of NGC 6819 led to the discovery of WOCS7017, a Li-rich red giant, a class that constitutes ∼1% of the red giant population (Deepak & Reddy 2019; Gao et al. 2019), located significantly redward and fainter than the red giant clump (Anthony-Twarog et al. 2013). Despite its CMD location, later spectroscopic and asteroseismic analysis (Carlberg et al. 2015; Handberg et al. 2017) demonstrated that this cluster member is a He-burning clump star of anomalously low mass.

The purpose of this study is to present preliminary analysis of a red giant with a unique combination of anomalous properties that collectively may have some bearing on the mechanism for retaining and/or enhancing Li abundances in stars well beyond the subgiant evolutionary phase. The star, WEBDA 2135 (W2135), is a member of the older (∼3.6 Gyr; Anthony-Twarog et al. 2005; Bragaglia & Tosi 2006; Twarog et al. 2020), metal-deficient ([Fe/H] ∼ −0.5; Anthony-Twarog et al. 2005; Jacobson et al. 2011; François et al. 2013; B. J. Anthony-Twarog et al. 2020, in preparation) cluster, NGC 2243. One prior estimate of [Fe/H] for W2135 exists, from Friel et al. (2002), a medium-dispersion spectroscopic study of several open clusters. Friel et al. (2002) obtain [Fe/H] = −0.50 for W2135, essentially identical to a cluster average of −0.49 that includes eight other giant members. The star is located approximately 2′.6 from the cluster center, placing it just within the radius containing 50% of the cluster members

[3] A(Li) = log$N_{\rm Li}$ − log$N_{\rm H}$ + 12.00.

($r_{50} = 2\farcm76$m; Cantat-Gaudin et al. 2018). As discussed below, W2135 is the reddest star at the level of the clump, a variable, and a single-lined, rapidly rotating, spectroscopic binary. In a cluster where the majority of giants have, at best, marginally detectable Li, W2135 falls just at or slightly below the defining boundary for Li-rich red giants.

2. Observational Data

2.1. Spectroscopy

Spectroscopic data were obtained using the WIYN 3.5 m telescope[4] and the Hydra multi-object spectrograph over two consecutive nights in 2015 January and one night in 2016 January. Details regarding the processing and reduction of these spectra will be presented in a future paper (B. J. Anthony-Twarog et al. 2020, in preparation), but follow the pattern laid out in previous cluster analyses such as NGC 6819 (Lee-Brown et al. 2015). All Hydra stars have been processed, stacked, and normalized in identical fashion. The final spectra for six member giants in our bright star configuration are the sums of three individual 30 minute exposures, producing a typical signal-to-noise ratio (S/N) of ∼140. Spectra for the fainter stars in our Hydra sample were constructed by taking nine separate exposures of 53 to 90 minutes in length and stacking them after processing to improve the S/N for each cumulative spectrum. W2135 was one of 13 member giants included in the faint star configuration. Because of its brightness, adequate S/N was achieved on each W2135 exposure, leading to an S/N of 315 for the cumulative Hydra spectrum.

These data were supplemented by spectra collected at the Very Large Telescope (VLT) using the Fibre Large Array Multi Element Spectrograph (FLAMES) fiber-feed assembly to the high-resolution UVES spectrograph and the GIRAFFE spectrograph, with pixel resolutions of 16.9 mÅ and 50 mÅ respectively. We searched for fully pipeline-processed spectra, initially restricted to spectra with S/N $\geqslant$ 70, that included the spectral range around 670 nm. The GIRAFFE spectra generally encompass a range of 640-680 nm while the higher resolution UVES spectra examined extend further to the blue (∼580 nm). For the VLT spectra examined and described here, typical S/Ns are 150.

2.2. Photometry and Astrometry

The primary photometric data set is that of Anthony-Twarog et al. (2005, hereafter ATAT), precision *uvbyCa*Hβ CCD photometry where the number of frames for the giant branch stars ranged typically from 10 for *y* to 24 for *u*. ATAT used the multicolor indices to identify highly probable cluster members and to convert the high precision (V, $b-y$) for likely members to the traditional (V, $B-V$) system defined by earlier, smaller CCD samples (Bonifazi et al. 1990; Bergbusch et al. 1991). The success of the approach is confirmed by Gaia DR2 (Gaia Collaboration et al. 2018), where astrometric analysis (Cantat-Gaudin et al. 2018) classifies 26 of the 28 ATAT giant members as definite cluster members, including W2135.

To make optimal use of all the cluster giants, we have transferred the Gaia DR2 (G, $B_p - R_p$) photometry to the (V, $B-V$) system discussed above using 25 member giants in common (W2135 excluded) to define quadratic relations in ($B_p - R_p$) between the two data sets and merged the two samples. The scatter in residuals between the two systems is ±0.007 mag and ±0.009 mag in V and ($B-V$), respectively. The transformation allowed the addition of 15 Gaia member giants not included in the ATAT survey, though one star has only a 20% membership probability.

As further validation of the DR2 photometry for W2135, we examined the quality factor defined by Evans et al. (2018), the `bprpexcess` factor. This factor summarizes a photometric consistency check among the B_p, R_p, and G passbands. For photometrically well-behaved sources, this factor should be under $1.3 + 0.06 * (B_p - R_p)^2$. For the case of W2135, this factor is 1.286, well below the color-based criterion of 1.399.

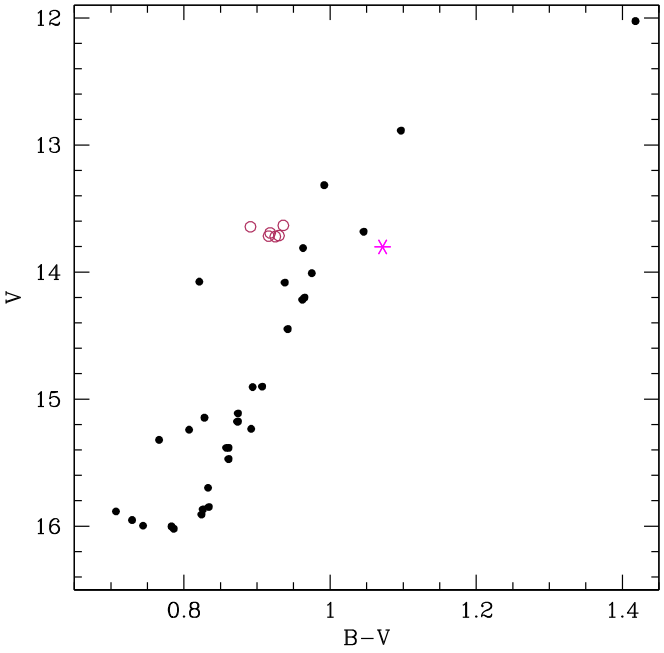

Figure 1. Color–magnitude diagram of the giant branch members of NGC 2243. Open circles denote red clump stars while star W2135 is a magenta asterisk.

3. Observational Peculiarities

As noted earlier, W2135 exhibits a number of photometric and spectroscopic peculiarities relative to typical stars at a similar state of evolution.

Figure 1 shows the CMD for the NGC 2243 member giants; for later reference, open circles identify the probable clump stars based on their CMD location, while the magenta asterisk tags W2135, clearly the reddest star at a luminosity which coincides well with that of the clump. W2135's standout position in the $b-y$ CMD of ATAT is similarly striking and is particularly noted in Figure 11 of that paper. Keeping the lesson of WOCS7017 in NGC 6819 in mind, the extreme color does not unambiguously determine if the star is a first-ascent giant or a He-burning member of the red clump. Equally important, while W2135 exhibits variability, discussed next, its CMD color in Figure 1 is based upon only two sources of photometry, the $b-y$ indices of ATAT and the $B_p - R_p$ Gaia DR2 indices transformed to a common $B-V$ system. Due to the photometric sequencing for the two data sets, the *b* and *y* frames always paired back-to-back

[4] The WIYN Observatory was a joint facility of the University of Wisconsin-Madison, Indiana University, Yale University, and the National Optical Astronomy Observatory.

for ATAT and B_p, R_p obtained simultaneously for Gaia, the redder CMD position compared to nonvariable giants at the same V level cannot be attributed to either a photometric error or magnitude differences triggered by filter observations collected at different phases of the light curve.
Noting its anomalously redder CMD location and systematically bluer m_1 and hk indices, ATAT were the first to suggest a potential variable nature for W2135, while expressing concern about possible photometric contamination from a faint nearby star. Even though the $uvbyCa\mathrm{H}\beta$ CCD survey was not designed with a variable star search in mind, the large number of frames in each color obtained in two observing runs 14 months apart clearly indicated photometric scatter in all filters at a level 2–3 times larger than other stars at the same luminosity. The variability range went from 0.09 mag for y to 0.15 mag in u, though the larger range in u may be a byproduct of a more extensive sample of u measures (24) versus y (9).

The variability was confirmed by Kaluzny et al. (2006a) as part of a search for variable stars with an emphasis on finding eclipsing binaries near the cluster turnoff. Of the dozen variables monitored by Kaluzny et al. (2006a), only two fell among the cluster giants, V11 (W1496) and V14 (W2135). Because of the luminosity of the giants, unsaturated exposures of these stars were achievable during only one run of five consecutive nights with a few hours of exposures per night. For W2135, a clear night-to-night decline over four nights followed by a slight rise in brightness on the fifth night, with a full range of at least 0.09 mag, is readily apparent. But, given the limited data, all one can say is that if a regular period exists it is more likely to be on a scale of days rather than hours. We will revisit the status of W1496 in Section 4.

Individual heliocentric stellar radial velocities, V_{RAD}, were derived from each summed composite Hydra spectrum utilizing the Fourier transform, cross-correlation facility *fxcor* in IRAF.[5] In this utility, program stars are compared to stellar templates of similar T_{eff} over the full wavelength range of our spectra excluding the immediate vicinity of the Hα line. Output of the *fxcor* utility characterizes the cross-correlation function, from which estimates of each star's radial velocity are easily inferred.

Continuing the pattern seen among the photometric variability measures, individual spectra of W2135 obtained on a given night over a few hours showed no identifiable differences within the uncertainties; the individual spectra required negligible wavelength shifts for alignment with each other. However, sets taken on consecutive nights of our first run required offsets of $\sim$2.5 km s^{-1} and stacked spectra taken over runs separated by a year required an offset of $\sim$35 km s^{-1}. The simple conclusion is that W2135 is a single-lined spectroscopic binary since no evidence of a second set of lines varying in opposition to the bright giant is readily apparent, keeping in mind the challenge of detecting the presence of a line set from a potentially much fainter companion star against the broad backdrop of the lines in W2135, as discussed below.

[5] IRAF is distributed by the National Optical Astronomy Observatory, which is operated by the Association of Universities for Research in Astronomy, Inc., under cooperative agreement with the National Science Foundation.

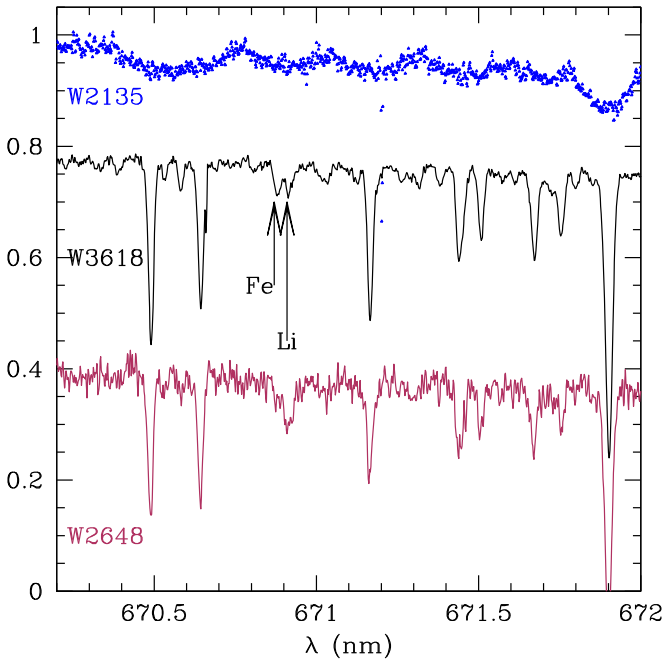

Figure 2. UVES spectra of three red giants in NGC 2243 highlighting the region of the Li line. All spectra are approximately normalized to a maximum level of 1.0; the plots for W3618 and W2648 are offset vertically downward for visibility.

One of the challenges of working with the spectra of W2135, and a potential reason for its absence from previous spectroscopic discussions of the cluster, is the exceptional broadness of its lines. Figure 2 illustrates the exceptional breadth of lines for W2135 by direct comparison between its UVES spectrum and UVES spectra for two giants with similar CMD locations. W3618 is positioned in Figure 1 at almost the same V mag level but slightly bluer than W2135. W2648 is located on the first-ascent RGB, fainter and bluer than W2135 and W3618 at $(V, B-V) = (14.45, 0.94)$. All three spectra are approximately normalized to the same level, with two of the spectra vertically offset for greater visibility in the plot.

The spectra illustrate the highest available spectral resolution with a range of S/N, highlighting the potential difficulties in separating the Li line from the nearby Fe I line at 6707.45 Å. The S/N for the three stars' spectra are 103, 192, and 65 for W2135, W3618, and W2648, respectively. With similar colors, all three stars should exhibit comparable Fe line strengths. While the two lines are clearly separable in the highest S/N spectrum of W3618, separation in the noisier spectrum for W2648 is less obvious although this star actually has a strong Li line. No separation is possible for the broad lines of W2135 irrespective of the S/N or spectral resolution.

From the procedure for radial-velocity estimation using Hydra spectra discussed above, rotational velocities can also be estimated from the cross-correlation function full width (CCF FWHM) using a procedure developed by Steinhauer (2003). This procedure exploits the relationship between the CCF FWHM, line widths and v_{ROT}, using a set of numerically "spun up" standard spectra with comparable spectral types to constrain the relationship. For simplicity, v_{ROT} as used here implicitly includes the unknown $\sin i$ term. From the Hydra

spectra for 18 red giant members, W2135 excluded, the mean v_{ROT} is $13.4 \pm 0.9\,km\,s^{-1}$ (sem). For W2135 the same procedure produces $38.8\,km\,s^{-1}$.

For the Hydra spectra, a majority of the line width for a normal giant is dominated by the instrumental line profile since the expectation is that most giants should be spinning in the range of 0–5 $km\,s^{-1}$. For simplicity, we will assume that the true v_{ROT} distribution for the giants should average such a small value, e.g., close to 1 $km\,s^{-1}$, and that the mean observed Hydra value for the red giants is equivalent to the instrumental profile. Under this assumption, the true v_{ROT} for W2135 is reduced to a minimum of $36.4\,km\,s^{-1}$.

The rare nature of these stars is confirmed by the findings of Carlberg et al. (2011) for ~1300 field K giants where 2.2% of the stars had v_{ROT} above $10\,km\,s^{-1}$ and only 5 stars had $v_{ROT} > 30\,km\,s^{-1}$. Tayar et al. (2015) found only 10 rapidly rotating stars in a sample of 1950 giants, none with v_{ROT} above 25 $km\,s^{-1}$. Three of these were in eclipsing binaries. A percentage comparable to that found by Carlberg et al. (2011) of 17377 Kepler giants have measurable rotation periods based upon starspot variability (Ceillier et al. 2017) with the intriguing caveat that for low-mass, red clump giants, typical of the clump stars in NGC 2243, the percentage may rise to 15%.

With the v_{ROT} derived above and its CMD position (luminosity and T_{eff}), the predicted rotation period for W2135 is ~15 days, significantly smaller than found among the typical rotating clump stars in Ceillier et al. (2017). Of 361 red giants with detectable rotation periods, only 17 have periods smaller than the W2135 value. It should be kept in mind that, unlike periods derived from photometric variability, the $\sin i$ term within v_{ROT} leads to, at best, an upper limit to the rotational period. The primary goals of the NGC 2243 study (B. J. Anthony-Twarog et al. 2020, in preparation; Twarog et al. 2020) are to probe the evolution of Li for stars at and above the cluster turnoff and to place NGC 2243 within the context of clusters of different age and metallicity. A comprehensive discussion of the derivation of A(Li) for all NGC 2243 giants, subgiants, and turnoff stars using equivalent width (EW) measures and spectrum synthesis will be detailed in B. J. Anthony-Twarog et al. (2020, in preparation). For current purposes and clarity, a simple approach using measured and published EWs can be usefully employed. As for previous studies, we employ splot, the graphical spectrum analysis tool in IRAF, to measure EWs and full-widths from Gaussian profile fits.

For previous investigations, we have used a computational scheme developed by Steinhauer (2003) and employed by Steinhauer & Deliyannis (2004) that interpolates within a model-atmosphere-based grid to translate EW values and temperature estimates based on unreddened $B - V$ colors into Li abundances, A(Li). For spectra inadequate to resolve the contribution of the nearby Fe I line at 6707.45 Å from the Li line at 6707.8 Å, the computational scheme also numerically subtracts a temperature and metallicity dependent estimate of the Fe line's contribution to the measured EW for the Li line. With the availability of UVES spectra for some of the giants, it has been possible to improve this color-based estimation of the Fe line contribution, and a correction of $(33.43 * \log(B - V)_0 + 16.44)$ mÅ has been applied to the measured EW for the Hydra and GIRAFFE spectra. EW′ reported for stars with UVES spectra denote the measured EW

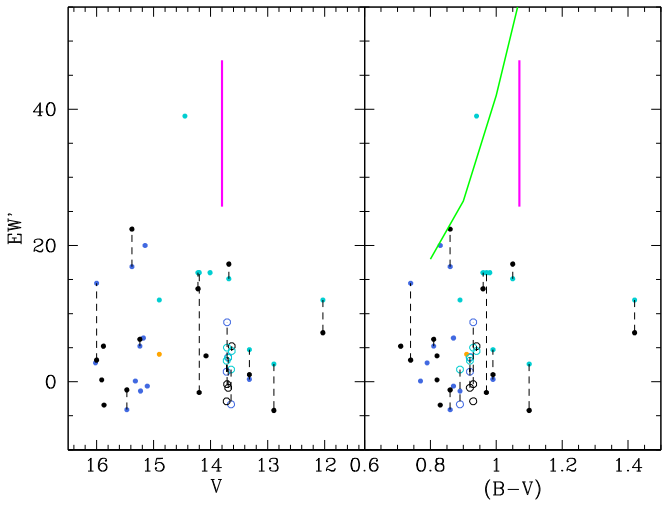

Figure 3. Corrected Li EWs for all giants from Hydra (black circles), GIRAFFE (blue circles), and UVES (teal circles) spectra. The filled orange circle is W1654. Open circles denote red clump stars. Measures for the same star from two sources of spectra are connected by dashed lines. The magenta band defines the spread in EW measures for W2135. The green line shows the expected EW′ values for stars with $A(\mathrm{Li}) = 1.0$ as a function of color.

of the Li line alone. In this computational scheme, as in future synthesis analyses, the color–temperature prescription of Ramírez & Meléndez (2005) is used for giants with an adopted value for $E(B - V) = 0.058$.

A key feature of the A(Li) abundance estimation scheme crafted by Steinhauer (2003) is its clear delineation of significant detections, for which the EW for the Li line alone must be at least three times the estimated error in the EWs, where the error is estimated from the spectrum resolution, the line full width and the S/N according to a prescription framed by Cayrel de Strobel (1988) and reformulated by Deliyannis et al. (1993). As detailed further below and in Figure 3, only a very few giants have EW′ that will imply a derived A(Li) detection. Moreover, the current computational scheme fails to extend to sufficiently cool temperatures and/or small EW′ values, a failing that will be addressed in B. J. Anthony-Twarog et al. (2020, in preparation).

Figure 3 shows the trend of Li EW′, the adjusted EW, with V and $(B - V)$. Measures from Hydra spectra are shown as filled black circles, with open circles denoting probable red clump stars. Measurements based upon spectra from GIRAFFE, with a resolution four times better than Hydra, are shown as filled blue circles, with open blue symbols for red clump stars. Data from the higher resolution UVES spectra are filled teal circles, with open teal circles signifying red clump stars. The one orange filled circle shows the corrected EW′ for W1654, based on the published EW (Hill & Pasquini 2000) and the color plotted in Figure 1. Stars with both VLT and Hydra spectra are connected by a vertical dashed line. Measured EW′ values for W2135 are plotted as a vertical magenta band to illustrate the potential range in EW′ for this star due solely to the difficulty in defining the level of the continuum for these very challenging spectra, whether Hydra or VLT, when attempting to derive the area contained by the line.

We note that the non-Hydra spectral measures include 12 of the 13 stars cooler than 5100 K listed for NGC 2243 in Magrini et al. (2017). It is assumed that these are the same 13 stars plotted in Figure 3 of Casali et al. (2019) but, unfortunately, no listing of their Li data is provided. Only 12 of the stars are

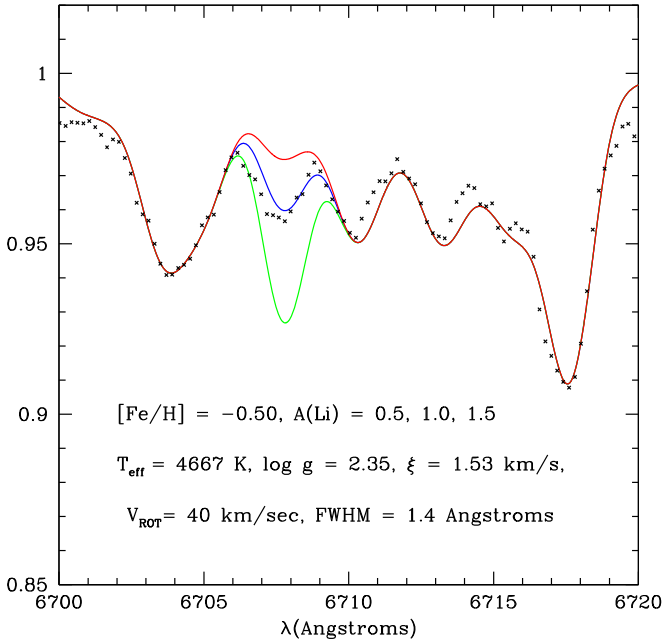

Figure 4. Hydra spectrum for W2135 compared to model spectra with A(Li) values of 0.5, 1.0, and 1.5.

included in our analysis because one of the cool giants listed by Magrini et al. (2017) within NGC 2243, W259, is a Gaia proper-motion and parallax nonmember.

Figure 3 also includes a green band showing presumptive EW′ values as a function of $B-V$ for stars with A(Li) = 1.0. Few of the giants and none of the clump stars approach this abundance value or have EW′ values above 15 mÅ. The light dashed lines joining measures for the same star illustrate the general agreement among spectroscopic samples with a range indicating an uncertainty of ∼5 mÅ.

One of the few stars with A(Li) potentially above 1.0 is W2648, as noted by François et al. (2013). Results from the UVES spectrum are shown in Figure 3 at (V, $B-V$, EW′ = 14.45, 0.94, 39). Referred to in their survey as K403, François et al. (2013) derive A(Li) = 1.5 for this star. Another star highlighted in their survey, W1261 (K1992), with Figure 3 coordinates (15.18, 0.87, 6.4), appears less likely to yield a detectable abundance from the GIRAFFE spectrum, so the abundance A(Li) = 1.24 cited by François et al. (2013) cannot be confirmed. Two other stars have EW′ values near the A(Li) = 1.0 locus for their color, W2613 (15.15, 0.83, 20) and W611 (15.38, 0.86, 16.9/22.4), with the higher EW′ value for W611 based on the Hydra spectrum.

Discussion of W2135 is clearly hampered by the large range of measured EW′ values. This range of measurement uncertainty is not attributable to inadequate S/N but to very uncertain continuum placement with respect to the extremely broad lines. We may gain additional insight into the Li abundance for this unique star by comparing its highest S/N spectrum, the lower resolution Hydra spectrum, to a model atmosphere spectrum in Figure 4. We employ the Kurucz (1992) models for [Fe/H] = −0.50, $T_{\rm eff}$ = 4667 K, with log g and microturbulent velocities appropriate for its giant branch location. The comparison was completed using the MOOG (Sneden 1973) software suite, with spectrum lines broadened to mimic the effect of a large rotational velocity, 40 km s^{-1}. Three values for A(Li) are shown in the figure, from which a value at or above 1.0 may be safely inferred for this star.

4. Implications and Future Needs

Taken separately, some of the anomalies—binarity, enhanced lithium, variability—exhibited by W2135 are found in other stars in the cluster. Rapid rotation appears to be unique to W2135. Variability of the type seen in W2135 is exhibited by W1496 (V11 in Kaluzny et al. 2006a). Binarity from photometry (Kaluzny et al. 2006a) and spectroscopy (Kaluzny et al. 2006b; François et al. 2013) has been detected among turnoff stars, but has only been inferred from supposedly anomalous CMD positions for some giants. As discussed above, W2135 is close to the limit for a Li-rich giant, but its high abundance is matched by one other giant within the cluster. The clear exception for W2135 is the rapid rotation rate, coupled with the mix of anomalies not found collectively in any other giant. It thus appears plausible that some, if not all, of the anomalistic characteristics of W2135 are linked directly or indirectly to its exceptional rotation.

Due to lower metallicity and thus a lower-mass Li dip, NGC 2243 bears a strong resemblance to the younger (2.25 Gyr) NGC 6819 (D19) in that stars populating the giant branch come from a narrow mass range just outside the Li dip. Adopting an age of 3.5 Gyr, [Fe/H] = −0.50 (B. J. Anthony-Twarog et al. 2020, in preparation), and the same isochrone set (VandenBerg et al. 2006) used to evaluate NGC 6819, stars leaving the main sequence in NGC 2243 are just below 1.24 $M_{\odot}$, while the precipitous decline in A(Li) defining the start of the Li dip occurs just below 1.21 $M_{\odot}$ (B. J. Anthony-Twarog et al. 2020, in preparation; Twarog et al. 2020). If NGC 2243 follows the pattern of other clusters, the $v_{\rm ROT}$ distribution of the current turnoff stars originally extended to 50 km s^{-1} or higher. The current mean $v_{\rm ROT}$ among turnoff stars is 16.2 ± 1.1 km s^{-1} (sem), with no star above 22 km s^{-1}, statistically identical to NGC 6819 (D19). As noted earlier, the giants, W2135 excluded, have an even smaller mean $v_{\rm ROT}$.

To explain the $v_{\rm ROT}$ of W2135 requires that either it:

> failed to spin down before exiting the main sequence or, it left the main sequence with low $v_{\rm ROT}$ but was spun up through internal or external evolutionary processes.

A comprehensive discussion of the many mechanisms proposed to explain rapid rotation (see, e.g., Carlberg et al. 2011) and/or Li enhancement in giants is well beyond the scope of this paper. Carlberg et al. (2011) have found that rapid rotation is more likely to occur among metal-poor and/or lower surface gravity giants, possibly due to the higher luminosity and larger radius at a fixed $T_{\rm eff}$ compared to a metal-rich giant, but triggered by interaction with a binary companion, possibly in a tidally locked system. For this reason and given the constraints imposed on W2135 by spectroscopy, we will narrow our focus to low-mass stars in binary systems.

If the current $v_{\rm ROT}$ for W2135 is indicative of the initial main-sequence $v_{\rm ROT}$, the expected rotational spindown and corresponding reduction of A(Li) as the star evolves through the subgiant and giant stages has been severely curtailed. This might be the case if W2135 is a short-period, tidally locked binary (SPTLB) since specific subclasses of these stars are known to retain high rotation and high levels of A(Li) (D19). Additionally, blue stragglers are commonly assumed to form via mass transfer (McCrea 1964) or stellar collisions (Leonard 1989), both of which can lead to stellar spinup while still on the main sequence. The challenge to these solutions is whether or not the evolved star retains the high $v_{\rm ROT}$ as it

evolves through the red giant phase. In the case of blue stragglers, the evidence appears to indicate that stars with these anomalies while on the main sequence spin down to a normal, low red giant v_{ROT} (Leiner et al. 2018), though synchronization triggered in SPTLBs evolving to the giant branch cannot be excluded.

If the visible giant left the main sequence with a normal reduction in v_{ROT}, its current exceptional v_{ROT} might imply a recent spinup via mass transfer while on the giant branch. Planetary engulfment can spin up a slowly rotating giant to v_{ROT} above 10 km s^{-1} (Carlberg et al. 2011), but the exceptional rotation rate of W2135 seems implausible for such a process. Moreover, engulfment is more likely to occur at the turnoff and on the lower giant branch while quickly dissipating the effects of any Li-enrichment in the upper giant branch (Soares-Furtado et al. 2020). When coupled with the significant V_{RAD} variation, the limited data point toward a recent mass transfer from a now low-luminosity object of stellar mass, possibly a post-asymptotic giant branch/white dwarf star.

While no other red giant in NGC 2243 studied to date exhibits the same panoply of characteristics as W2135, it should be noted that the second variable star tagged by Kaluzny et al. (2006a), V11 (W1496), has all the nonspectroscopic markings found in the primary rapidly rotating candidate. The V11 light curve shows an amplitude of at least 0.05 mag over a range of a few days, with too few data points to be more specific since the star was only monitored over one five-night run. In the earlier ATAT study, W1496 shows larger scatter than expected for its V magnitude, again in all filters, but was not highlighted as a potential variable since the range in variation was not as extreme as that found for W2135. Its location in the CMD, if it had been plotted in Figure 1, would be at (V, $B-V$)=(15.6, 0.73), near the base of the vertical RGB, but bluer that expected for its V magnitude or, equivalently, a subgiant brighter than expected for its color. It shows the same anomalous colors in m_1 and hk as W2135, being too blue for its $b-y$, by more than 0.2 mag in hk (see Figure 8 in ATAT where W1496 has ($b-y$, hk) = (0.50, 0.49)). Despite the anomalous position, W2135 was retained by ATAT as a member because its radial velocity was consistent with membership, a designation later confirmed by both proper motions and parallax from Gaia DR2. By contrast, no spectroscopy has been obtained for W1496 and, surprisingly, the star has not been included to date within the Gaia astrometric data set, which may explain its absence from more recent spectroscopic surveys. If its membership can be confirmed either spectroscopically or astrometrically, W1496 would join the three stars between $V=15$ and 16 which clearly lie blueward of the first-ascent giant branch, indicative of some form of anomalous origin and/or evolution relative to a normal single star within the cluster.

We close by noting some potential observational avenues for clarifying the state of the W2135 system. Abundance anomalies normally supply signatures for mass transfer events and key ionized lines might provide hints about the surface gravity and thus the stellar mass, but the exceptional broadness of the lines in W2135 (Figure 2) illustrates the challenge to this approach. The key to resolving the unusual nature of W2135 lies with the companion. A complete light curve would distinguish between eclipses and/or rotationally defined star-spot cycles as the predominant origin of the variability. If rotation causes variability, the period would constrain the true v_{ROT} and set the inclination of the system. If eclipses can be detected, one can constrain the properties of the companion and, in conjunction with V_{RAD} measures over the orbital cycle, define the mass.

We gratefully acknowledge the helpful comments of the referee which led to valuable clarification of the technical aspects of the spectra and their analysis. NSF support for this project was provided to B.J.A.T. and B.A.T. through NSF grant AST-1211621, and to C.P.D. through NSF grants AST-1211699 and AST-1909456. Extensive use was made of the WEBDA database maintained by E. Paunzen at the University of Vienna, Austria (http://www.univie.ac.at/webda). This research has made use of the services of the ESO Science Archive Facility and is based on observations collected at the European Southern Observatory under ESO program 188.B-3002(V).

Facility: WIYN:3.5m.

Software: IRAF Tody (1986), MOOG Sneden (1973).

Note added in proof. It has been recently noted that W2135 was included in the All-Sky Automated Survey for SuperNovae (ASAS-SN) variable stars data base (Shappee et al. 2014). The cataloged star, ASASSN-V J062941.11-311906.9/V0412 CMa, is classed as ROT, meaning the variability is likely due to rotationally-induced brightness modulation, with a period of 6.755421 days (Jayasinghe et al. 2019). With the stellar parameters discussed in Section 3, this observed period implies a true VROT of 86 km s^{-1}, validating the extreme nature of this exceptional binary red giant.

ORCID iDs

Barbara J. Anthony-Twarog https://orcid.org/0000-0001-8841-3579
Constantine P. Deliyannis https://orcid.org/0000-0002-3854-050X
Bruce A. Twarog https://orcid.org/0000-0001-5436-5206

References

Anthony-Twarog, B. J., Atwell, J., & Twarog, B. A. 2005, AJ, 129, 872
Anthony-Twarog, B. J., Deliyannis, C. P., Rich, E., & Twarog, B. A. 2013, ApJL, 767, L19
Anthony-Twarog, B. J., Deliyannis, C. P., & Twarog, B. A. 2016a, AJ, 148, 51
Anthony-Twarog, B. J., Deliyannis, C. P., & Twarog, B. A. 2016b, AJ, 152, 192
Anthony-Twarog, B. J., Deliyannis, C. P., Twarog, B. A., Croxall, K. V., & Cummings, J. 2009, AJ, 138, 1171
Anthony-Twarog, B. J., Deliyannis, C. P., Twarog, B. A., Cummings, J. D., & Maderak, R. M. 2010, AJ, 139, 2034
Anthony-Twarog, B. J., Lee-Brown, D. B., Deliyannis, C. P., & Twarog, B. A. 2018, AJ, 155, 138
Bergbusch, P. A., VandenBerg, D. A., & Infante, L. 1991, AJ, 101, 2102
Boesgaard, A. M., Lum, M. G., & Deliyannis, C. P. 2020, ApJ, 888, 28
Boesgaard, A. M., & Tripicco, M. J. 1986, ApJL, 302, 49
Bonifazi, F., Fusi Pecci, F., Romeo, G., & Tosi, M. 1990, MNRAS, 245, 15
Bragaglia, A., & Tosi, M. 2006, AJ, 131, 1544
Cameron, A. G. W., & Fowler, W. A. 1971, ApJ, 164, 111
Cantat-Gaudin, T., Jordi, C., Vallenari, A., et al. 2018, A&A, 618, 93
Carlberg, J. K., Majewski, S. R., Patterson, R. J., et al. 2011, ApJ, 732, 39
Carlberg, J. K., Smith, V. V., Cunha, K., et al. 2015, ApJ, 802, 7
Casali, G., Magrini, L., Tognelli, E., et al. 2019, A&A, 629, A62
Cayrel de Strobel, G. 1988, in IAU Symp. 132, The Impact of Very High S/N Spectroscopy on Stellar Physics, ed. G. Cayrel de Strobel & M. Spite (Dordrecht: Kluwer), 345
Ceillier, T., Tayar, J., Mathur, S., et al. 2017, A&A, 505, A111
Cummings, J. D., Deliyannis, C. P., Anthony-Twarog, B. J., Twarog, B. A., & Maderak, R. M. 2012, AJ, 144, 137

Cummings, J. D., Deliyannis, C. P., Maderak, R. M., & Steinhauer, A. 2017, AJ, 153, 128
Deepak, & Reddy, B. E. 2019, MNRAS, 484, 2000
Deliyannis, C. P., Anthony-Twarog, B. J., Lee-Brown, D. B., & Twarog, B. A. 2019, AJ, 158, 163
Deliyannis, C. P., Pinsonneault, M. H., & Duncan, D. K. 1993, ApJ, 414, 740
Evans, D. W., Riello, M., DeAngeli, F., et al. 2018, A&A, 616, A4
François, P., Pasquini, L., Biazzo, K., Bonifacio, P., & Palsa, R. 2013, A&A, 552, A136
Friel, E. D., Janes, K. A., Tavarez, M., et al. 2002, AJ, 124, 2693
Gaia Collaboration, Brown, A. G. A., Vallenari, A., et al. 2018, A&A, 616, A1
Gao, Q., Shi, J.-R., Yan, H.-L., et al. 2019, ApJS, 245, 33
Handberg, R., Brogaard, K., Miglio, A., et al. 2017, MNRAS, 472, 979
Hill, V., & Pasquini, L. 2000, in IAU Symp. 198, The Light Elements and Their Evolution, ed. L. Da Silva, J. R. de Medeiros, & L. Spite (San Francisco, CA: ASP), 293
Jacobson, H. R., Friel, E. D., & Pilachowski, C. A. 2011, AJ, 141, 58
Jayasinghe, T., Stanek, K. Z., Kochanek, C. S., et al. 2019, MNRAS, 486, 1907
Kaluzny, J., Krzeminski, W., Thompson, I. B., & Stachowski, G. 2006a, AcA, 56, 51
Kaluzny, J., Pych, W., & Rucinski, S. M. 2006b, AcA, 56, 237
Kurucz, R. L. 1992, in Proc. IAU Symp. 149, The Stellar Populations of Galaxies, ed. B. Barbuy & A. Renzini (Dordrecht: Kluwer), 225
Lee-Brown, D., Anthony-Twarog, B. J., Deliyannis, C. P., Rich, E., & Twarog, B. A. 2015, AJ, 149, 121
Leiner, E., Mathieu, R. D., Gosnell, N. M., & Sills, A. 2018, ApJL, 869, L29
Leonard, P. J. T. 1989, AJ, 98, 217
Magrini, L., Randich, S., Kordopatis, G., et al. 2017, A&A, 603, A2
McCrea, W. H. 1964, MNRAS, 128, 147
Pinsonneault, M. 1997, ARA&A, 35, 557
Ramírez, I., & Meléndez, J. 2005, ApJ, 626, 465
Ryan, S. G., & Deliyannis, C. P. 1995, ApJ, 453, 819
Shappee, B. J., Prieto, J. L., Grupe, D., et al. 2014, ApJ, 788, 48
Smiljanic, R., Franciosini, E., Bragaglia, A., et al. 2018, A&A, 617, A4
Sneden, C. 1973, ApJ, 184, 839
Soares-Furtado, M., Cantiello, M., MacLeod, M., & Ness, M. K. 2020, arXiv:2002.05275
Steinhauer, A. 2003, PhD thesis (Indiana Univ.)
Steinhauer, A., & Deliyannis, C. P. 2004, ApJL, 614, L65
Tayar, J., Ceillier, T., García-Hernández, D. A., et al. 2015, ApJ, 807, 82
Tody, D. 1986, Proc. SPIE, 627, 733
Twarog, B. A., Anthony-Twarog, B. J., Deliyannis, C. P., & Steinhauer, A. 2020, MmSAI, 91, 74
VandenBerg, D. A., Bergbusch, P. A., & Dowler, P. D. 2006, ApJS, 162, 375